Using deformation modes to identify cracks in turbine engine compressor disks

[†]R. A. Brockman
Robert.Brockman@udri.udayton.edu
[‡]R. John
Reji.John@WPAFB.AF.MIL
[†]M. A. Huelsman

[‡]US Air Force Research Laboratory
Materials and Manufacturing Directorate, AFRL/RXLMN
Wright-Patterson Air Force Base
Ohio, USA

[†]University of Dayton Research Institute
Dayton, Ohio, USA

ABSTRACT

Recent studies show that analytical predictions of crack growth in rotating components can be used in conjunction with displacement measurement techniques to identify critical levels of fatigue damage. However, investigations of this type traditionally have focused on the detection of damage at known flaw locations. This paper addresses the related problem of estimating damage associated with flaws at unknown locations, through the combined use of analytical models and measured vibration signatures. Because the measured data are insufficient to identify a unique solution for the location and severity of fatigue cracks, the function of the analytical model is to bound the extent of damage occurring at life-limiting locations. The prediction of remaining life based on estimates of worst-case fatigue damage and crack locations also is discussed.

1.0 INTRODUCTION

Monitoring of structural integrity is an area of broad interest, encompassing civil structures[1,2], aerospace vehicle structures[3,4], and engine systems for power generation and propulsion[5,6]. Each of these areas provides unique challenges in terms of instrumentation, data collection, pattern recognition, and analytical modeling. The most significant progress has been made in structural health monitoring of aerospace and civil structures, in which it is often feasible to employ numerous sensors, and the process of data collection and analysis is in many respects straightforward. Turbine engines present particularly difficult challenges in health monitoring, since the thermal environment is hostile, the components of interest are mostly rotating, and the flow path must remain unobstructed. For this reason, most engine health monitoring efforts have been limited to the detection or monitoring of cracking in shafts[7-9].

Certainly the most significant challenges in engine health monitoring are logistical, since the environment inside a turbine engine places severe limitations on the number and type of sensors that might be used. However, some possibilities do exist, in the form of temperature sensors, blade-tip clearance or arrival time measurements from capacitive probes, and magnetostrictive gauges attached to the shaft or other lower-temperature surfaces. Ground-based measurements conducted between flights, and off-wing measurements performed during maintenance work, may be used to augment the dynamic measurements made in service. The life management of turbine engine disks is one of the more attractive applications of material prognosis technology, since these components are expensive to replace, difficult to inspect, and required to operate in complex and hostile loading environments that dictate a highly conservative retirement philosophy. The ability to monitor the damage state of such components *in situ*, project subsequent damage development, and estimate remaining life would be revolutionary in terms of cost savings, safety, and fleet readiness[10-12]. Presently, developments in engine health monitoring are of greatest interest to

Paper No. 3347. Manuscript received 18 September 2008, accepted 15 May 2009.

https://doi.org/10.1017/S0001924000003468 Published online by Cambridge University Press

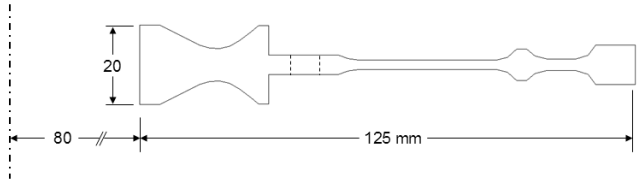


Figure 1. Generic disk model cross section.

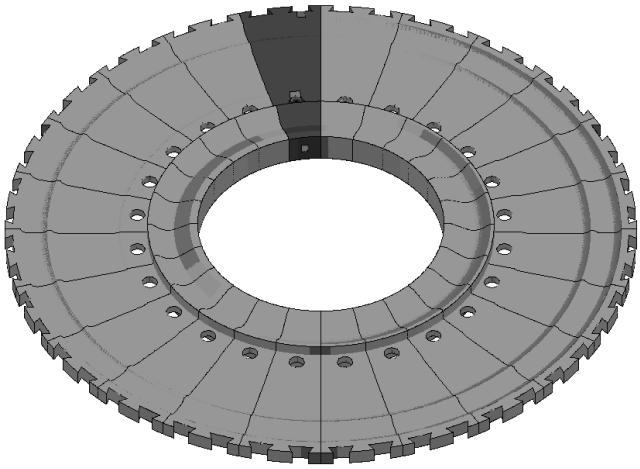


Figure 2. Substructured generic disk model.

defense customers, to minimise sustainment costs; however, the prospect of selling 'power by the hour' to commercial customers may soon provide equally great incentives to the propulsion industry.

Recent experiments on actual turbine disk hardware confirm that it is indeed feasible to detect and identify increasing damage using a combination of indirect measurements and analytical models, at least in the context of full-scale spin pit experiments (c.f. Fig. 5 of Ref. 5). Recent experimental work[5,13] also suggests that the prospects for damage detection in rotating components are significantly improved by averaging measured responses over a large number of cycles, and by signature monitoring based on prior knowledge of the damage modes of interest.

In what follows, we discuss the use of analytical models to provide accurate information for use in the pattern recognition process leading to damage detection. Since our examples involve rotating turbine disks, the specific form of damage of interest is fatigue crack initiation and growth. The methods described have been used successfully in investigations of crack growth in rotating disks, and corroborated by experimental evidence[5]. As a practical matter, such studies invariably involve production or prototype hardware whose characteristics are business sensitive, export controlled, or both, and cannot be presented in detail in the open literature. In the interest of presenting the analytical methodology we have used for crack detection and monitoring in studies of actual hardware, we have created a notional rotor system to demonstrate the logic and procedures employed, if only in the setting of a paper study.

In what follows, we use a model of an idealised compressor stage to demonstrate a process for identifying damage in the disk, bounding the likely crack size, and estimating key parameters such as the current stress intensity factor and fatigue crack growth rate. Our focus is on the analytical models needed to make the proper connections between remotely measured data and localised response at a probable damage site.

The present study uses an idealised compressor disk model in which known damage states, in the form of cracks in high-stress locations, are introduced to simulate the data normally taken experimentally. This pseudo data is generated for a series of cracks of arbitrary size, and subsequently treated as if only the resulting displacement values are known, with the crack locations and sizes to be determined by the analytical procedure. Additional models of the disk are applied as usual, to estimate perturbations in the displacements caused by hypothetical cracks of various sizes in strategic locations. The resulting 'library' of displacement perturbations is used in an identification procedure to infer the probable location and size of cracks in the pseudo data from the hypothetical damaged rotor. Both the accuracy and the conservative or non-conservative nature of these predictions (in the sense of bounding) are of interest, since ultimately we wish to predict the remaining life of the component.

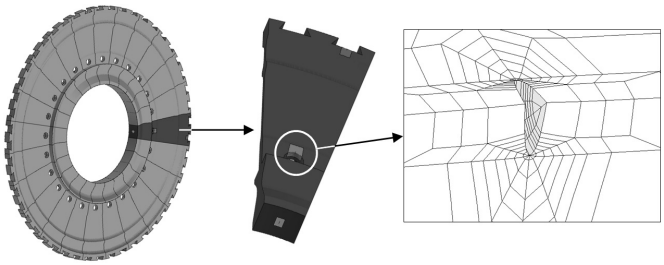


Figure 3. Complete disk, possible crack locations within a sector, and local mesh detail.

It should be noted that significant questions exist about the feasibility of performing adequate displacement measurements in such systems. While we have been successful in monitoring crack development in spin-pit experiments, the amplitude of response perturbations caused by crack growth in a realistic engine setting may be significantly different. This paper does not address measurement issues; however, experimental investigations now in progress will, we hope, provide further guidance on sensor requirements and related practical issues. Additional refinements to the analysis methodology are certainly possible in some areas, such as signal analysis and probability estimation[14,15].

2.0 DISK MODEL

Our model of a generic engine disk possesses geometric, mass, and stiffness characteristics typical of a compressor disk, but is not based on a particular production component. In the present study, we simplify the model by representing the blades only by pressures in the slots, and monitoring displacement values in the blade posts. The disk has an inner radius of 80mm, outer radius of 205mm, and varies in thickness between 2·5 and 20mm (Fig. 1). The mechanical properties are typical of a Ni-base superalloy (E = 200GPa, ν = 0·30, ρ =8,300kg/m^3). Most of the results that follow correspond to a nominal rotation speed of 10,000RPM.

The complete disk model consists of 24 identical sectors, represented by copies of a single substructure spanning 15 degrees of arc (Fig. 2). Each sector contains a single 10mm hole in the web, and two blade slots. This configuration is a bit more 'analyst friendly' than most actual disk hardware, and allows liberal use of substructuring in the construction of cracked and uncracked models of the disk. The procedure used for less regular geometries is identical, except for the fact that the geometry modelling is somewhat more laborious.

It should be noted that the analyses performed in the present study also are simplified in that there is no consideration of residual stress, temperature, contact, plasticity, and similar phenomena that figure prominently in investigations of actual hardware under realistic operating conditions. Here we limit the response calculations to linear elastic analysis in the interest of demonstrating the overall methodology. In the analysis of actual rotor hardware, some or all of

https://doi.org/10.1017/S0001924000003468 Published online by Cambridge University Press

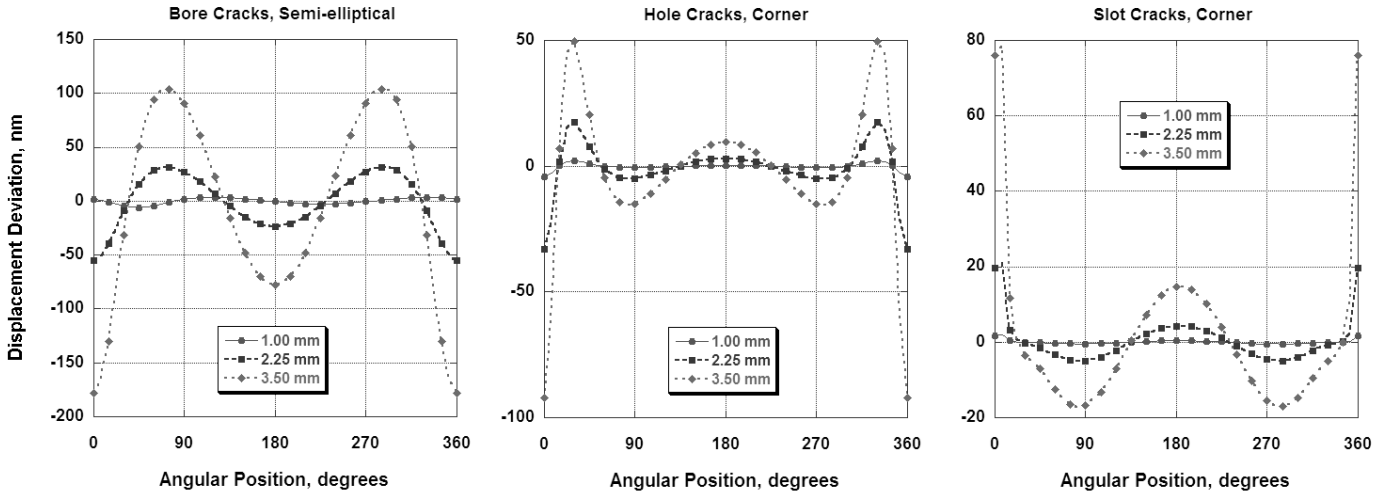


Figure 4. Analytical signatures for radial displacements in known crack configurations: (a) bore; (b) web hole; (c) blade slot.

these features must be included in the analytical predictions to achieve satisfactory accuracy.

To introduce a crack in any sector of the disk, we create a modified version of the basic substructure in which the crack is introduced. We have used the Zencrack[16] software to generate focused meshes with quarter-point finite elements surrounding the crack tip, as shown in Fig. 3. The centre pane of Fig. 3 shows the typical crack locations considered here, namely the disk bore, the edge of the hole in the web, and the blade slot bottom. The use of the detailed crack tip mesh, shown in the right-hand pane of Fig. 3, allows the extraction of accurate stress intensity factor data in the cracked area(s).

A complete disk model containing a single crack consists of 23 identical uncracked substructures and a single cracked substructure. The external nodal connections in the cracked and uncracked sectors are identical; therefore, introducing one or more cracks is as simple as specifying a different substructure name to replace an uncracked sector. Multiple cracks located in separate sectors can be defined by identifying the appropriate (cracked) substructure models as needed. Multiple cracks, or variations in crack size, within a single sector require a new substructure definition, which becomes part of the component database and may be reused as needed. All analyses are performed using ABAQUS[17].

3.0 CRACK SIGNATURES

Because the present study involves both analytical signature data, and measured data that are simulated using an analytical model, we hope to reduce the possibility for confusion by adopting highly specific terminology that will be used throughout. We will refer to analytically predicted crack deformation patterns for simple cracks in known locations and of given size as analytical crack signatures. We will use the term measured signature to describe pseudo data that, in the study of an actual system, would be collected through experimental observations. In the present study, this measured data is created using an analytical model of the disk, with cracks introduced in arbitrary locations with randomly selected crack lengths. However, the 'measured' signature data contain crack locations and sizes that are not represented in the analytical crack signature data. In the context of a similar study using actual hardware, the analytical signature data represents displacement or other patterns generated for a particular component using existing design-analysis models, and stored in a component-specific database for later reference; the measured signature data correspond to field measurements collected during testing, in service, or during routine maintenance.

It is worth mentioning that the signatures in question consist of discrete response values at locations where measurements might be taken. The response data making up each analytical signature are obtained by performing a static analysis of the disk under steady-state operating conditions. In generating the analytical signature data, it may be advisable to extract displacements, strains, or other values of potential interest at many locations, if the actual measurement locations are not known in advance. Likewise, it may be useful to collect multiple components of vectorial or tensorial quantities to suit more than one sensor configuration; for instance, 'tip displacement' measurements might involve either tip clearance (radial) components or time of arrival (combined axial and circumferential) components.

Analytical crack signature data have been created for single cracks of various sizes in the disk bore, at the edge of the hole in the web, and in the base of a blade slot. As mentioned earlier, this data, which will be used to identify the location and size of cracks from the 'measured' data, normally would be generated using design-analysis models of the component, by introducing cracks analytically at high-stress locations, in orientations of highest potential interest, and with various lengths. The analytical bore crack is elliptical, and located in the axial center of the bore. The hole and slot cracks are idealised as semicircular corner cracks. In each location, analytical crack signatures corresponding to crack lengths of 1·00, 2·25, and 3·50mm have been predicted, providing a small library of analytical signatures for specific damage types (Fig. 4). In each case, the crack is located in the sector of the disk having one edge at an angular position of zero degrees. In all cases, the signatures characterising damaged states of the disk consist of values of displacement deviations, or differences between the measured displacement and the steady-state value for the undamaged system.

The displacement deviations that make up the signature for a given crack condition may include both positive and negative displacements. A negative displacement deviation means simply that the displacement amplitude at a particular point on the rotor is smaller when passing a given sensor location than the corresponding value in the undamaged disk. Negative values occur because a crack at a given location causes an overall distortion of the disk, which involves varying amounts of radial displacement as one looks around the circumference of the disk. Some locations exhibit radial expansion while others contract. Strain values are a useful indicator of the deformation, but are far more difficult to measure, and are more meaningful when the entire distribution can be viewed, rather than values at a few selected points. Displacements at key points (blade tips, posts, etc.) at least give an indication of the overall

https://doi.org/10.1017/S0001924000003468 Published online by Cambridge University Press

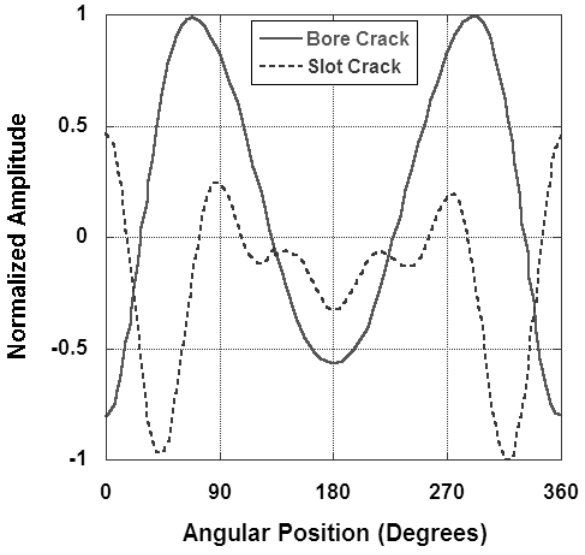


Figure 5. Displacement amplitudes from model of fielded disk.

deformation pattern of the disk circumference, which is very useful information.

Notice that the signatures for cracks in various locations are distinctive, in the sense that they each involve quite different combinations of displacement harmonic components. Note also that for the slot cracks, which are very near the sensor location, the peaks in the signatures are more highly localised, while those further inboard exhibit more gradual amplitude variations. In general, the farther outboard the crack location, the more localised the displacement pattern will be. The amplitude of the signature for a given crack type varies nonlinearly with crack size. Corresponding to each analytical displacement signature in the library, in addition to the crack size and location, we retain a value of the corresponding stress intensity factor for use in crack growth estimation. If a measured signature can be identified using a series of conditions in the analytical database, it is possible not only to estimate a crack size, but also to interpolate for the corresponding stress intensity factor and the corresponding crack growth rate using the material crack growth behaviour, i.e. crack growth rate versus stress intensity factor range relationship.

The phase offset of a damage signature can be used to estimate the circumferential location of a crack. If an observed crack signature resembles one of the analytical crack signature patterns, but is shifted in phase from the analytical signature, the phase difference provides an indication of the position of the sector in which the observed crack is located.

While the present disk model is highly idealised, the damage signature characteristics predicted by the model and used in the study are similar to those observed in fielded systems. Figure 5 shows typical signature data for a model of an actual bladed disk, for nominally-sized cracks in the bore and blade slot bottom. The slot crack signature for the idealised model exhibits somewhat more localised response than the actual system, but the character of the displacement patterns is quite reasonable. In practical applications of the methodology described in this paper, it is feasible to introduce additional signature data for a given component during the service life of the part, as performance and inspection data become available.

It should be noted that several types of probes are commonly used for sensing blade tip position, based on capacitance, eddy current, and optical measurements. The probe may be positioned to give blade tip clearance in the radial or axial directions, or time of arrival. As such, it is possible to sense deflection patterns in terms of radial, circumferential, axial, or combined components of displacement. The choice of probe type, position and orientation is constrained by the geometry of the stage and the available space; in some situations, the magnitude of the displacements caused by blade vibration may overwhelm any evidence of damage elsewhere in the stage, dictating the use of a very specific sensor position and orientation. Figure 6 shows comparisons of signatures based on radial (clearance) and tangential (arrival time) displacement data for a single disk. Notice that the amplitude of each signature has been normalised using the steady state radial displacement. Two cycles of each trace are shown in the figure to make the patterns easier to discern. The displacement signatures for a particular damage location are distinctive, but the amplitudes and detailed character of the radial and tangential traces are different for each crack location.

4.0 MULTIPLE-DISK SYSTEMS

A word is in order regarding the magnitudes of the displacement deviations in the signature plots of Figs 4 through 6. While the displacement magnitudes are quite small, it should be noted that the data are obtained from a model of a single disk only, rather than of the complete rotor system. In a model of the disk alone, the asymmetry in response caused by the stiffness perturbation in the cracked disk cannot be determined, since it depends on the mass and stiffness characteristics of the complete rotordynamic system. Instead, one must artificially constrain the displacement corresponding to the shaft whirl mode to stabilise the model against rigid-body displacement. Unfortunately, the whirl displacement component is one of the most significant artifacts of the damage in the real system. In a single-disk model we are limited to analysing the higher-order harmonic components, which are quite small. In the tests described in Ref. 5, it was indeed possible to measure the asymmetric displacement components and to correlate the measured signatures with analytical predictions of the probable damage mode. Thus, there is real evidence that such a measurement is achievable, at least in the setting of a spin pit test.

Additional analyses have been performed using models that depict the stiffness and mass properties of the surrounding system in an approximate way. Figure 7 shows the displacement amplitude associated with a slot bottom crack in one disk, mounted on a shaft with two identical disks, as the shaft stiffness varies. The nominal shaft size J_{nom} corresponds to conditions observed in spin tests of similar components. The far right end of the plot, where the damage-related displacement amplitudes are extremely small, corresponds to a single-disk model. In the one-disk model, the mean and whirl displacements are constrained to eliminate rigid-body motion of the model. For the multiple-disk model on an extremely stiff shaft, damage to a particular disk produces no whirl displacement component because the remainder of the system is so stiff, and the energy penalty associated with any displacement perturbation in the stiffer portion of the system is prohibitively large.

The signatures in Fig. 8 correspond to the same system shown in Fig. 7, with the shaft size at its nominal value. The characteristic displacement patterns are somewhat more localised, and actually slightly larger in amplitude, than those shown in Fig. 6 for the single-disk model.

The upshot of these examples is that the displacements culled from a single-disk model are always artificially small, and the true amplitudes will be a complicated function of the stiffness and mass characteristics of the complete system. Attempts to characterise damage conditions in terms of simplistic concepts like ‘mass imbalance’ fail to acknowledge the complex interactions of all components in the highly-coupled rotordynamic system.

https://doi.org/10.1017/S0001924000003468 Published online by Cambridge University Press

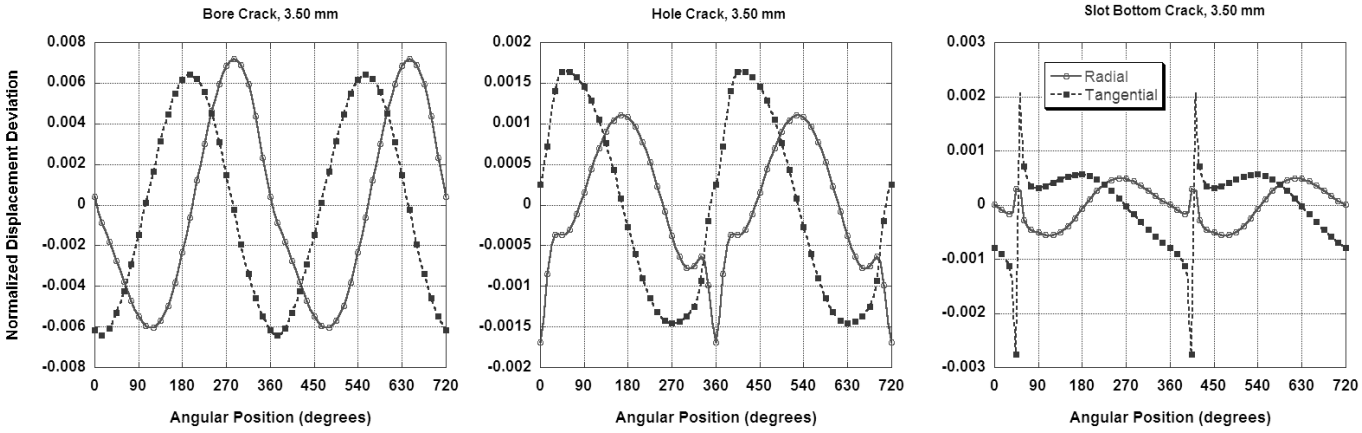


Figure 6. Comparison of radial and tangential displacement signatures for various crack locations in a single disk.

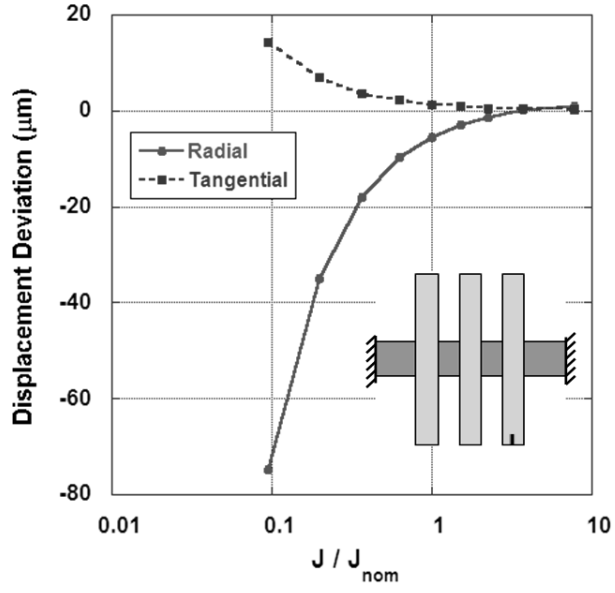


Figure 7. Displacement amplitude variation with shaft stiffness.

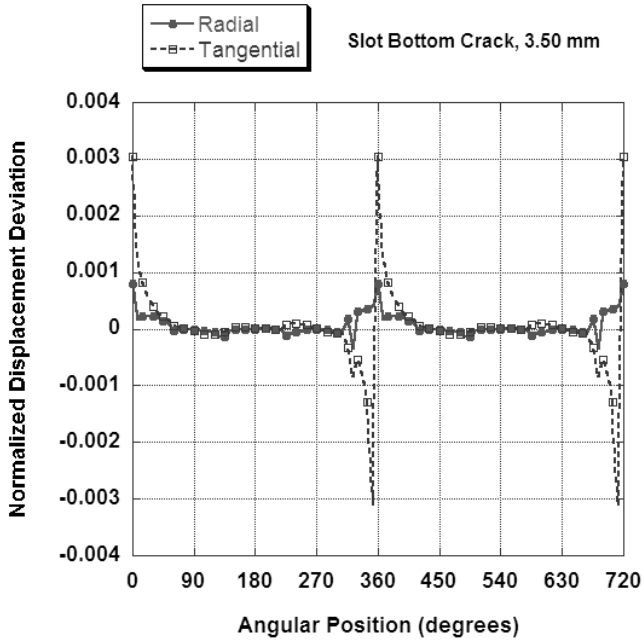


Figure 8. Displacement signatures due to damage in neighbouring disks.

It is also worth mentioning that the presence of other rotating hardware attached to the disk may affect the magnitude and character of disk damage signatures in several ways. The mass of a disk seal may amount to a significant fraction of the disk weight, thereby affecting the dynamic impedance of the system. If a seal is highly stressed, vibratory motions caused by damage in the seal may dominate the measured signal, making the process of identification more difficult.

Clearly, the issue of whether damage-induced motions can be measured successfully in specific systems remains a pivotal issue, in terms of the role an onboard measurement system might play in monitoring the integrity of the system and providing useful information about remaining life. Further experimental investigation of realistic rotor systems is needed to establish the feasibility of measuring response data with sufficient accuracy for damage mode identification.

5.0 SIGNATURE FILTERING AND PROCESSING

In this investigation, we will assume that a blade tip clearance sensor, such as a capacitance or eddy current probe, is used to collect radial displacement data from the disk. Therefore, the damage modes are characterised by the deviation of the radial displacement from the nominal steady-state value. In the single disk model used for most of the calculations, the first harmonic of the radial displacement, which corresponds to the rigid-body shaft whirl displacement of the disk, is purely an artifact of the model constraints and is filtered out of the results. The procedures we describe for analysing the measured data are general, and would be identical if the first harmonic components were present.

https://doi.org/10.1017/S0001924000003468 Published online by Cambridge University Press

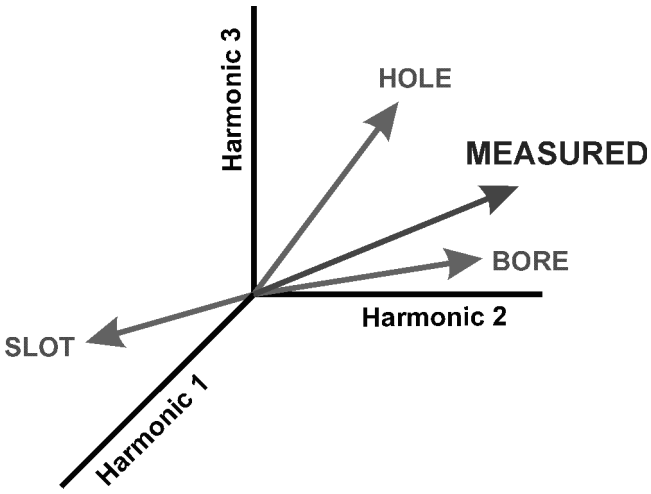


Figure 9. Simplified diagram of signature patterns in harmonic co-ordinate space.

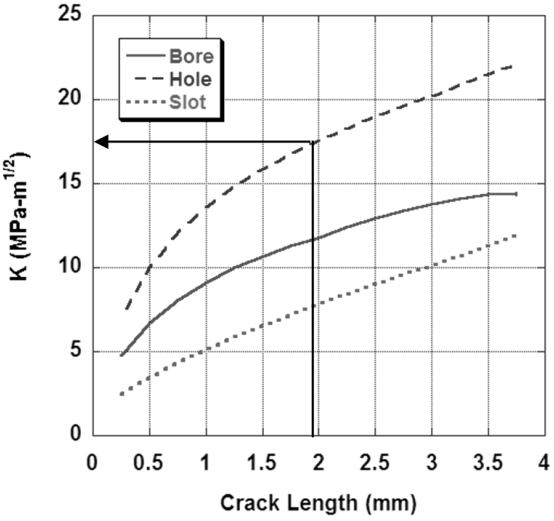


Figure 11. Stress intensity factor estimate from crack length.

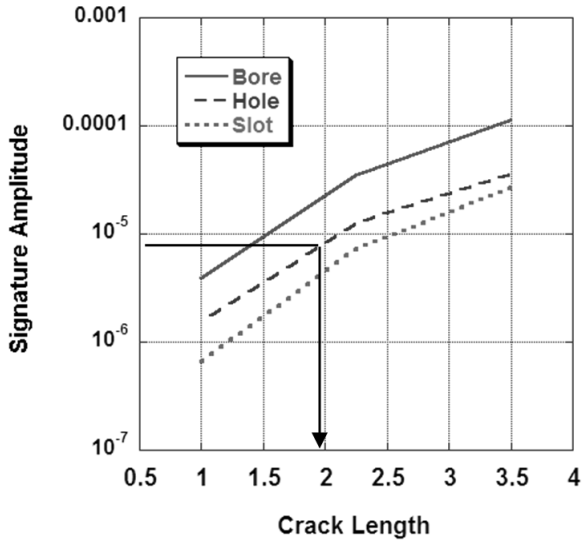


Figure 10. Inverse interpolation for estimated crack length.

For both the analytical and 'measured' signatures, we begin the characterisation of a given signature by calculating finite Fourier transforms of the radial displacement data. The displacement amplitude in sector 'i' of the disk can be expressed in the form

$$U_i = U_0 + \sum_{k=1}^{N} A_k \,\mathrm{Cos}\frac{2\pi k}{N}(i-1) + B_k \,\mathrm{Sin}\frac{2\pi k}{N}(i-1) \qquad \ldots (1)$$

in which A_k and B_k are the Fourier coefficients. The number of components, N, is determined by the number of equally-spaced measurement locations around the circumference of the disk. The magnitude of the kth harmonic component is $C_k = \sqrt{A_k^2 + B_k^2}$

Equation (1) may be rewritten in terms of amplitude and phase as

$$U_i = U_0 + \sum_{k=1}^{N} C_k \,\mathrm{Cos}\left[\frac{2\pi k}{N}(i-1) - \varphi_i\right] \qquad \ldots (2)$$

The relative magnitudes of the harmonic components C_k are significant in determining the type of damage mode under consideration (e.g., crack location), while the absolute magnitudes are important in determining the extent of the damage (crack size). The phase differences (related to the ratios A_k/B_k) indicate the location of the damage site around the circumference of the disk.

We first characterise the signature by its direction in the space of harmonic co-ordinates,

$$\mathbf{d} = \frac{\mathbf{C}}{\sqrt{\mathbf{C} \bullet \mathbf{C}}} \qquad \ldots (3)$$

in which $\mathbf{C} = \{C_1, C_2, C_3, \ldots, C_n\}^T$ is an N-dimensional vector of harmonic amplitudes. Figure 9 shows a notional sketch of this scheme, using only three harmonic components. In this step, both the measured signal and analytical damage signatures are normalised to unit magnitude, giving the direction vectors

$$\mathbf{d}_{\mathrm{MEAS}} = \frac{\mathbf{C}_{\mathrm{MEAS}}}{\sqrt{\mathbf{C}_{\mathrm{MEAS}} \bullet \mathbf{C}_{\mathrm{MEAS}}}} \qquad \ldots (4a)$$

$$\mathbf{d}_{\mathrm{k}} = \frac{\mathbf{C}_{\mathrm{k}}}{\sqrt{\mathbf{C}_{\mathrm{k}} \bullet \mathbf{C}_{\mathrm{k}}}};\ k = 1, 2, \ldots, M \qquad \ldots (4b)$$

Here M is the number of analytical crack signatures used for the damage identification; increasing the number of analytical signatures improves the accuracy of the identification process, in general. The projection of the measured signal onto each of the reference signatures is computed, from the inner products

$$P_k = \mathbf{d}_{\mathrm{k}} \bullet \mathbf{d}_{\mathrm{MEAS}};\ k = 1, 2, \ldots, M \qquad \ldots (5)$$

Equations (4) eliminate the absolute magnitude and phase data, while retaining the information about the relative magnitude of the harmonic components, thus making it easier to identify the damage type; in the case of cracking in a turbine disk, the remaining information helps to identify a crack in terms of generic location (bore, hole, slot). The 'nearest neighbours' of the measured signal, corresponding to the largest values among the projections P_k, are selected as candidates for further analysis. It should be noted that Fig. 9 is highly simplified, in the sense that signatures for similar cracks of different sizes at a given location do not point in precisely the same direction, but do tend to cluster in a relatively small region of the harmonic space.

https://doi.org/10.1017/S0001924000003468 Published online by Cambridge University Press

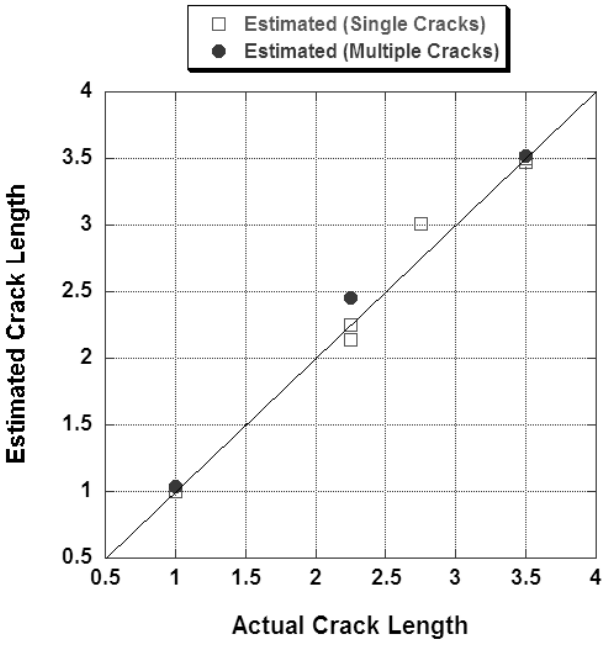


Figure 12. Crack length estimates from nearest neighbours in harmonic co-ordinate space.

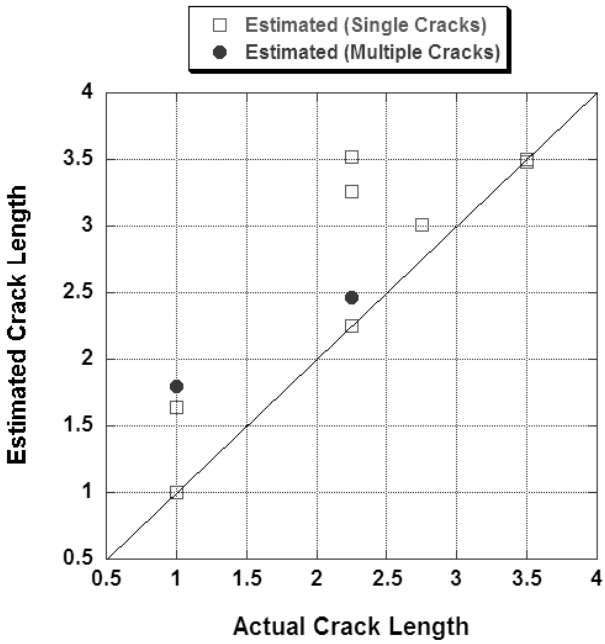


Figure 13. Crack length estimates based on multiple neighbours in harmonic co-ordinate space.

For each analytical signature exhibiting a sufficiently large projection P_k on the measured signal, a series of signatures is extracted from the database for similar cracks of different sizes, for use in interpolation. Figure 10 shows a simple example in which the signal amplitudes of bore, hole, and slot bottom cracks of various sizes might be used to estimate crack length for a given signal amplitude. Frequently, more than one of these groups might be used to obtain a crack length estimate for a single measured signal, particularly when multiple cracks are present. Once the estimated crack length has been determined, one can interpolate from the corresponding data for stress intensity factors to obtain estimates of K and the corresponding crack growth per cycle (Fig. 11).

6.0 DAMAGE IDENTIFICATION

Damage estimates have been performed for numerous cases, with the 'measured' signature data being generated using substructured models similar to those used to generate analytical signature data. The models used to generate 'measured' signatures contain cracks of different sizes and in different locations from the analytical signature data, as well as sectors with multiple cracks. Simulated disk measurements have been generated for configurations with single cracks, multiple cracks in a single sector, and multiple cracks in different sectors, for crack sizes different from those represented in the database of analytical crack signatures.

Crack length estimates based on selection of the single analytical signature closest to the measured signature in harmonic space ('nearest neighbour') are shown in Fig. 12. Notice that the crack length estimates are quite accurate, but in some cases the estimates are non-conservative bounds (that is, the crack length is underestimated). The reason for this is that some estimates, especially for multiply-cracked disks, will have been based on crack types or locations that are inexact. Using several near-neighbour signatures to make multiple estimates does result in conservative predictions, as shown in Fig. 13. In practice, one would expect to augment the database of analytical signatures for a given component as time progresses, allowing the predictions to converge on the correct crack size and location after several successive measurements. A second benefit of this approach is that the tolerances applied to select specific signatures for use in damage estimates almost certainly can be reduced as more damage conditions are added to the database, giving a sharper estimate of the location and extent of damage associated with the dominant defect. Following the determination of the crack size and location, the remaining crack growth life of the component can be predicted as discussed next.

7.0 PREDICTION OF REMAINING CRACK GROWTH LIFE

Given a reasonable body of crack growth performance data for the material(s) of interest, useful estimates may be made for the probable crack growth rate and remaining fatigue crack growth life of the component of interest. In the examples below, we analyse the same disk model described in Section 2, operating at 18,000RPM, with stress ratio $R = 0{\cdot}10$.

To obtain a more accurate relationship between crack size and stress intensity factor for use in the life prediction, a series of 16 models has been analysed for each crack configuration for crack lengths between 0·125mm and 3·75mm. In each case, a cubic polynomial fit is used to describe the stress intensity factor range versus crack length (ΔK-a) relationship (Fig. 14). Note that $\Delta K = K_{max}*(1\text{-}R)$, where K_{max} = stress intensity factor at maximum RPM. To predict the propagation of cracks as a function of loading cycles, the relationship between crack growth rate ($\mathrm{d}a/\mathrm{d}N$) and stress intensity factor range (ΔK) is assumed to be given by

$$\frac{\mathrm{d}a}{\mathrm{d}N} = C\,\Delta K^{n} \qquad \ldots (6)$$

Here the stress intensity factor range has units of $MPa\sqrt{m}$, crack growth rate is in mm/cycle, $C = 5{\cdot}0 \times 10^{-11}$mm/cycle and $n = 3{\cdot}70$. For simplicity, the same values C and n are assumed to be applicable

https://doi.org/10.1017/S0001924000003468 Published online by Cambridge University Press

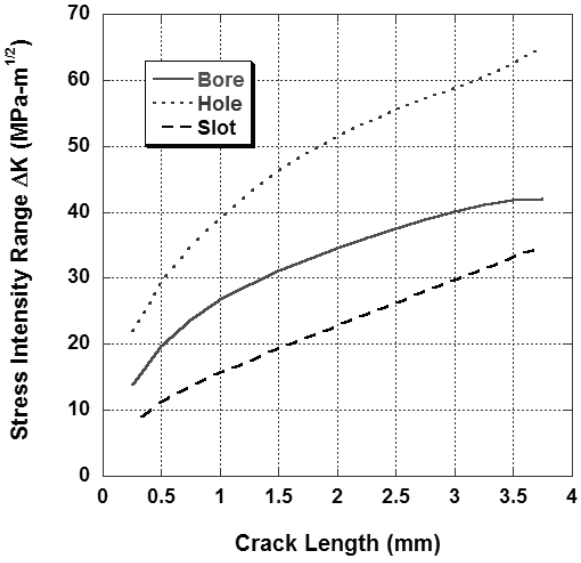


Figure 14. Polynomial fits for ΔK as a function of crack length.

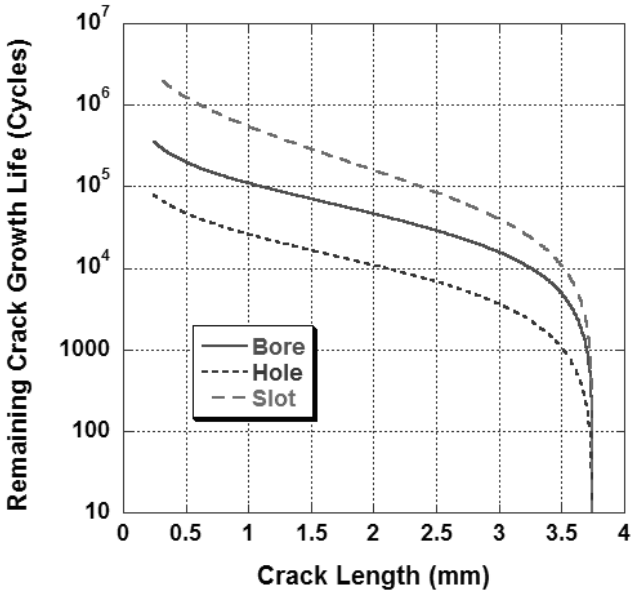


Figure 15. Remaining crack growth life as a function of crack length.

at the bore, hole and slot locations. These values of C and n correspond to a powder metallurgy Ni-base superalloy, Udimet 720 [18]. However, in general, C and n can be expected to be dependent on stress ratio, temperature, environment and microstructure, and would be determined experimentally for specific operating conditions of interest.

Equation 6 can be reformulated as

$$N = \int_0^a \frac{\mathrm{d}a}{C\,\Delta K^n} \qquad \ldots (7)$$

giving a relationship between crack length and number of cycles for crack propagation. For the purpose of prognosis, i.e. prediction of future performance, the remaining crack growth life, NREM is obtained by integrating between the current crack length ('a' as estimated from the signal analysis) and the critical crack length (a_c),

$$N_{REM} = \int_a^{a_c} \frac{\mathrm{d}a}{C\,\Delta K^n} \qquad \ldots (8)$$

The critical crack length a_c is assumed to be 3·75mm for this example calculation. Figure 15 shows the predicted remaining crack growth life as a function of crack length for the three potentially critical locations. For crack lengths greater than 3·4-3·5mm, the decrease in remaining life is very steep. Hence, the accuracy of the estimate for the current crack length becomes quite important as the crack length approaches the critical value.

8.0 SUMMARY AND CONCLUSIONS

A substructure-based analytical testbed has been created to demonstrate a methodology used for identification of cracking damage in turbine engine disks. The substructuring approach makes it relatively simple to model damaged regions in detail, thereby allowing estimates not only of crack location and size, but also of stress intensity factors and likely crack growth rates. Identification of the damage modes in a measured signature is accomplished by analysing the Fourier-transformed signature and that of several analytically predicted signatures residing in a database for the component of interest. The direction of the transformed signal in harmonic space indicates the probable type and location of the crack; using a series of analytical signatures for different-length cracks of the same type, estimates of the crack size can be obtained through interpolations based on the amplitude of the measured signal.

A particularly important use of the present methodology is in refining one's estimate of the type, location, and extent of damage as data become available at successive times. In the process, additional relevant crack locations and sizes for the component can be analysed and added to the database, to sharpen the estimation of the probable damage condition.

The methodology presented here demonstrates the key analytical elements of a prognosis system for fracture critical components such as disks, based on the integration of damage signature information and crack growth life prediction models. In practice, the use of such a system for asset management will require the generalisation of the current deterministic methodology to provide probabilistic risk assessment.

Further analyses of multiple-disk systems, as well as experimental investigations, are needed to establish the feasibility of measuring displacement data to the accuracy required for reliable assessment of damage evolution in fielded engine disks. The consideration of blade vibrations is a further area of interest because of the rich harmonic content that is introduced into the measured data. Depending on the characteristics of particular systems, it may be possible to monitor disk damage, blade damage, or both from a given type of motion sensor. The feasibility of each of these options must be assessed for specific systems, to define a logical approach for managing the remaining life of the complete system.

ACKNOWLEDGEMENT

This work was performed at the Air Force Research Laboratory, Materials and Manufacturing Directorate, AFRL/RXLMN, Wright-Patterson Air Force Base, OH, USA, under on-site Contract No. FA8650-04-C-5200. The authors gratefully acknowledge the support of Dr Leo Christodoulou of the Defense Advanced Research Projects Agency (DARPA) under DARPA order S271 and Dr Victor Giurgiutiu of the Air Force Office of Scientific Research (AFOSR) under task 2306-6M2AL8. We are grateful also to the reviewers of the original manuscript for numerous useful comments and suggestions.

https://doi.org/10.1017/S0001924000003468 Published online by Cambridge University Press

REFERENCES

1. KO, J.M. and NI, Y.Q. Technology developments in structural health monitoring of large-scale bridges, *Engineering Structures*, October 2005, **27**, (12), pp 1715-1725.
2. CHANG, P.C., FLATAU, A. and LIU, S.C. Review paper: health monitoring of civil infrastructure, *Structural Health Monitoring*, September 2003, **2**, (3), pp 257-267.
3. GIURGIUTIU, V., ZAGRAI, A.N. and BAO, J. Piezoelectric wafer embedded active sensors for aging aircraft structural health monitoring, *Structural Health Monitoring*, July 2002, **1**, (1), pp 41-61.
4. TAKEDA, N., TAJIMA, N., SAKURAI, T. and KISHI, T. Recent advances in composite fuselage demonstration program for damage and health monitoring in Japan, *Structural Control and Health Monitoring*, December 2005, **12**, (3-4), pp 245-255.
5. VON FLOTOW, A., TAPPERT, P., MERCADAL, M. and HARDMAN, W. Successes and failures for LCF rotor burst prognosis using blade tip sensors, 2004, Paper GT-2004-54131, Proceedings ASME Turbo Expo 2004, Vienna, Austria, June 2004.
6. SAAVEDRA, P.N. and CUITIÑO, L.A. Vibration analysis of rotor for crack identification, *J Vib and Control*, 2002, **8**, pp 51-67.
7. GASCH, R. A survey of the dynamic behavior of a simple rotating shaft with a transverse crack, *J Sound Vib*, November 1993, **160**, (2), pp 313-332.
8. HE, Y., GUO, D. and CHU, F. Using genetic algorithms and finite element methods to detect shaft crack for rotor-bearing system, *Math Comp Simulation*, 2001, **57**, pp 95-108.
9. GOUNARIS, G.D. and PAPADOPOULOS, C. Crack identification in rotating shafts by coupled response measurements, *Eng Frac Mech*, 2002, **69**, pp 339-352.
10. LARSEN, J.M. and CHRISTODOULOU, L. Integrating damage state awareness and mechanism-based prediction, *J Materials*, March 2004, **56**, (3) p 14.
11. CHRISTODOULOU, L. and LARSEN, J.M. Using materials prognosis to maximize the utilization potential of complex mechanical systems, *J Materials*, March 2004, **56**, (3), pp 15-19.
12. KACPRZYNSKI, G.J., SARLASHKAR, A., ROEMER, M.J., HESS, A. and HARDMAN, W. Predicting remaining life by fusing the physics of failure modeling with diagnostics, *J Materials*, March 2004, **56,** (3), pp 29-35.
13. RUSS, S.M., ROSENBERGER, A.H., LARSEN, J.M., BERKELEY, R.B., CARROLL, D., COWLES, B.A., HOLMES, R.A., LITTLES, J.W., PETTIT, R.G. and SCHIRRA, J.J. Demonstration of advanced life-prediction and state-awareness technologies necessary for prognosis of turbine engine disks, *Health Monitoring and Smart Nondestructive Evaluation of Structural and Biological Systems III*, 2004, Proceedings SPIE Conference on Smart Structures and Materials NDE for Health Monitoring and Diagnostics, San Diego, California, UK, March 2004.
14. SEKER, S., AYAZ, E. and TÜRKCAN, E. Elman's recurrent neural network applications to condition monitoring in nuclear power plane and rotating machinery, *Eng Appl Art Intelligence*, 2003, **16**, pp 647-656.
15. SEIBOLD, S. and WEINERT, K. A time domain method for the localization of cracks in rotors, *J Sound Vib*, 1996, **195**, (1), pp 57-73.
16. *Zencrack User's Manual*, Version 7.1, September 2003, Zentech International, Camberley, Surrey, UK.
17. *ABAQUS Analysis User's Manual*, Version 6.7, 2007, Dassault Systèmes, Providence, Rhode Island, USA.
18. LUO, J. and BOWEN, P. Small and long fatigue crack growth behavior of a PM Ni-based superalloy, Udimet 720, *Int J Fatigue*, 2004, **26**, (2), pp 113-124.

https://doi.org/10.1017/S0001924000003468 Published online by Cambridge University Press